

# Collective dynamics and phase transition of active matter in presence of orientation adapters

Sagarika Adhikary and S. B. Santra

Department of Physics, Indian Institute of Technology Guwahati, Guwahati-781039, Assam, India.

E-mail: a.sagarika@alumni.iitg.ac.in, santra@iitg.ac.in

**Abstract.** In this work, the orientation adapter, a species of active particles that adapt their direction of motion from the other active particles, is introduced. The orientation adapters exist besides the usual Vicsek-like particles; both are self-driven, however, follow different interaction rules. We have studied the dynamics in high speed of the particles keeping dissimilar speeds for these different species. The effect of orientation adapters on the collective behaviour of the system is explored in this model. The orientational order-disorder phase transition is mainly studied in such systems. First, for equal density of both species, when the adapter speed  $v_a = 1.2v_0$  and usual particles speed  $v_0 = 1.0$ , both adapters and the usual particles form dense travelling bands and move in the same direction. Near the transition point, such bands appear and disappear over time, giving rise to the co-existence of two phases. The adapters and the usual particles both undergo a discontinuous transition. The nature of the transition is further confirmed by the existence of hysteresis in the order parameter under a continuously varying noise field. However, when the adapter velocity becomes much higher than the usual SPPs  $v_a \approx 7v_0$ , the formation of travelling bands disappears from the system, and the transition becomes continuous. The density ratio is also varied, keeping the velocities constant, and the phase transition is studied. For a high adapter velocity with  $v_a = 10v_0$ , the continuous transition is found with low-density values of the adapters. The critical exponents related to the continuous transition are also determined.

## 1. Introduction

Active or self-propelled particles (SPPs) are known for self-organisation and collective motion. Fish schools [1, 2, 3], flocking birds [4, 5], mammalian herds [6], human crowd [7, 8], swarms of insects [9, 10, 11, 12], bacteria swarms [13, 14, 15], cell clusters [16], actin filaments inside our cells [17, 18], and even many artificial self-driven systems [19, 20, 21] are all examples of active matter which exhibits collective motion. In a seminal work, Vicsek *et al.* proposed a model for studying the collective motion of SPPs in two dimensions, known as the Vicsek model (VM). In this model, a large number of SPPs move together at a constant speed ( $v_0$ ), and they align their direction of motion with their neighbours through a short-range interaction. However, it is subject to an angular noise ( $\eta$ ), present in the system. For a given density ( $\rho_0$ ), an orientational order-disorder transition occurs at a critical noise ( $\eta_c$ ). Initially, the nature of this phase transition in the VM was found to be continuous for low velocity on small system sizes [22, 19]. However, later it is established through extensive simulations that there exists a crossover system size  $L^*(\rho_0, v_0)$  [23, 24] below which the order of the transition is continuous, and above which it is discontinuous where dense bands appear in the system. It needs to be

noted that  $L^*(\rho_0, v_0)$  diverges both for low velocities ( $v_0 < 0.05$ ) and low densities ( $\rho_0 < 0.01$ ) [23]. The formation of the dense travelling band near the transition region is fluctuation-driven and occurs due to the feedback mechanism between local order and local density [25].

One of the major characteristics of the VM is that all the SPPs have the same speed, and they all interact with each other locally. However, in natural systems, the velocities of particles need not be the same, and also there can be some other type of species which interact differently. In a recent study of collective dynamics in a binary mixture of SPPs with widely different velocity [26, 27], interesting collective patterns and nontrivial phase transitions are observed. Collective dynamics are studied with variable speeds of SPPs, which depend on the neighbourhood's polarization [28, 29]. Apart from velocities, other properties of active particles are also varied in many systems. Examples of such systems include: a mixture of SPPs with different sizes [30], a mixture of active Brownian particles with different diffusion constant [31, 32], a mixture of active and passive particles [33, 30, 34, 35], binary active particles with different alignment interactions [36], an oppositely driven binary mixture of particles [37, 38, 39], chiral active matter [40, 41], a mixture of polar and apolar SPPs [42] and many others. However, the study mixture of species with different interaction properties in the polar SPPs is a relatively new area of research. The effect of another type of species, we call them orientation adapters, on the collective behaviour of usual SPPs, is a crucial aspect to study in the context of the VM. The orientation adapters are the species that adapt their direction of motion from other SPPs. We have proposed a model where adapter SPPs exist besides the usual SPPs in equal or smaller proportions. The adapter SPPs do not interact among themselves but adopt the velocity orientation of the usual SPPs through local interactions. However, the usual SPPs do interact with themselves as well as with the adapters. The model implements not only different alignment interaction rules, moreover, their velocities will be dissimilar. It will be interesting to investigate the effect of adapters on the order-disorder transition phase transition. What would be the nature of such a transition? In this study, we explore all these questions as the adapters induce nontrivial collective behaviour in the system.

## 2. The Model

A mixture of usual SPPs with adapter SPPs is modelled over a two-dimensional square box of linear size  $L$  with periodic boundary conditions. The usual SPPs move with a velocity  $v_0$ , and the adapter SPPs move with velocity  $v_a$ . They are taken in equal proportion. If  $N_0$  is the number of usual SPPs and  $N_a$  is the number of adapters, then  $N_0 = N_a = N/2$  (only for the case with same proportion of the two species), where  $N$  is the total number of SPPs in the system. Initially, the position  $\vec{r}_{p,i}$ ,  $i = 1, 2, 3, \dots, N/2$  of all the SPPs are randomly distributed over the space where  $p \in \{0, a\}$ . The initial orientation  $\theta_{p,i}$  of an SPP is randomly selected in the range  $-\pi$  to  $\pi$ , irrespective of their type. The usual SPPs interact within a local neighbourhood  $R = 1$  and determine their average orientation. Whereas an adapter only interacts with usual SPPs within the local neighbourhood  $R = 1$  and determine their average orientation.

The distribution of 25 randomly oriented usual SPPs (in orange) and 25 randomly oriented adapters (in indigo) are shown in Fig.1. Longer and shorter arrows show the velocities  $v_a$  and  $v_0$ , respectively as in this case  $v_a > v_0$ . The circular region of radius  $R$  indicates the region of interaction.

The time evolution of the orientation  $\theta_{0,i}$  of an usual SPP is determined by

$$\theta_{0,i}(t + \Delta t) = \langle \theta(t) \rangle_{R \in \{0, a\}} + \Delta \theta \quad (1)$$

Where, The interaction term  $\langle \dots \rangle_{R \in \{0, a\}}$  for usual SPPs includes both the usual SPPs (0) and the adapters (a) within the radius  $R$ . Whereas, time evolution of the orientation  $\theta_{a,i}$  of an

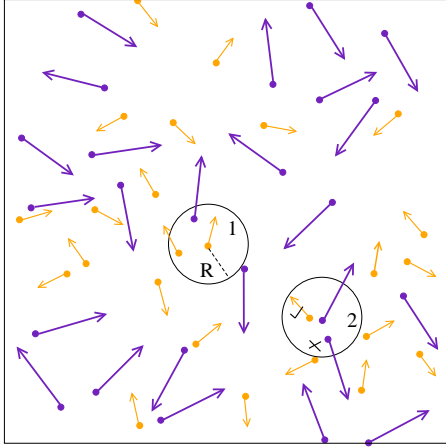


**Figure 1.** The distribution of the SPPs are shown on a square box of size  $L = 10$  where  $N_0 = N_a = 25$ . The orange colour represents usual SPPs, and the indigo colour represents the adapters. The arrow associated with an SPP indicates its orientation, and here  $v_a > v_0$ . A usual SPP present at the centre of circle-1 interacts with both SPPs present within the circle of radius  $R$ . Whereas an adapter SPP at the centre of circle-2 interacts only with usual SPPs present within the circle of radius  $R$ .

adapter is determined by

$$\theta_{a,i}(t + \Delta t) = \langle \theta(t) \rangle_{R \in \{0\}} + \Delta \theta \quad (2)$$

where, the interaction term  $\langle \dots \rangle_{R \in \{0\}}$  for adapters only include the usual SPPs within the radius  $R$ . It should be noted that the magnitude of the velocity of individual SPPs is ignored and only the orientations are taken into account in estimating  $\langle \theta(t) \rangle_R$  for both the usual SPPs and the adapters. Here,  $\Delta \theta$  is a random orientation chosen with a uniform probability from the interval  $[-\eta\pi, +\eta\pi]$ . The strength of the angular noise  $\eta$  varies from 0 to 1 and act as a control parameter. After averaging, an SPP of type- $p$  ( $p \in \{0, a\}$ ) at the position  $\vec{r}_{p,i}$  is thus moving with a speed  $v_p$  in the direction  $\theta_{p,i}$ . Knowing the velocity  $\vec{v}_{p,i}(t)$  at every time step, the position of the  $i$ th SPP  $\vec{r}_{p,i}$  is updated following the forward update rules as given below

$$\vec{r}_{0,i}(t + \Delta t) = \vec{r}_{0,i}(t) + \vec{v}_{0,i}(t)\Delta t \quad (3)$$

$$\vec{r}_{a,i}(t + \Delta t) = \vec{r}_{a,i}(t) + \vec{v}_{a,i}(t)\Delta t \quad (4)$$

where  $\Delta t$  is the time between two successive updates, and it is chosen as  $\Delta t = 1$ . Eqs.1, 2, 3 and 4 are then evolved with time and dynamical properties of the model are studied, varying  $\eta$  for different velocity ranges.

### 3. Phase transition and Finite-size scaling

Now, we present the results of the orientational order-disorder phase transition for this model. We analyze the data for the whole system, considering both types of SPPs together, as well as the partial systems involving only one type of SPPs. The order parameter of the transition  $\phi$  for the whole system is defined as

$$\phi(\eta, L) = \frac{1}{N} \left| \sum_p \sum_{i=1}^{N_p} \frac{\vec{v}_{p,i}}{|\vec{v}_{p,i}|} \right| \quad (5)$$

where  $N$  is the total number of SPPs. The partial order-parameter of the transition  $\phi_p$  for the  $p$ -type SPPs is defined as

$$\phi_p(\eta, L) = \frac{1}{N_p} \left| \sum_{i=1}^{N_p} \frac{\vec{v}_{p,i}}{|\vec{v}_{p,i}|} \right| \quad (6)$$

where  $N_p$  is the number of  $p$ -type ( $p \in \{0, a\}$ ) SPPs.

The susceptibility  $\chi$  for the whole system and that of the partial systems  $\chi_p$  can be estimated from the fluctuation in their respective order parameters  $\phi$  and  $\phi_p$  as

$$\chi = L^2 [\langle \phi^2 \rangle - \langle \phi \rangle^2], \quad \chi_p = L^2 [\langle \phi_p^2 \rangle - \langle \phi_p \rangle^2] \quad (7)$$

where  $\langle \phi^n \rangle = \int \phi^n P(\phi) d\phi$ ,  $\langle \phi_p^n \rangle = \int \phi_p^n P(\phi_p) d\phi_p$ ,  $P(\phi)$  and  $P(\phi_p)$  are the distribution functions of  $\phi$  and  $\phi_p$  respectively. Similarly, the fourth-order Binder cumulant for the whole system and that of the partial systems are defined as,

$$U = 1 - \frac{\langle \phi^4 \rangle}{3\langle \phi^2 \rangle^2}, \quad U_p = 1 - \frac{\langle \phi_p^4 \rangle}{3\langle \phi_p^2 \rangle^2} \quad (8)$$

where the higher-order averages are obtained following the definitions of  $\langle \phi^n \rangle$  and  $\langle \phi_p^n \rangle$  given above.

If the orientational order-disorder transition is continuous, the finite size scaling (FSS) relations of the above parameters can be given following equilibrium critical phenomena [43, 44], as

$$\phi(\eta, L) = L^{-\beta/\nu} \phi_0[\epsilon L^{1/\nu}] \quad (9)$$

where  $\epsilon = (\eta - \eta_c)/\eta_c$  the reduced noise,  $\beta$  is the order parameter exponent,  $\nu$  is the correlation length exponent and  $\phi_0$  is a scaling function. At the criticality  $\eta = \eta_c$ ,  $\phi(\eta_c, L) \sim L^{-\beta/\nu}$ . The order parameter distribution  $P_L(\phi)$  for a given system of size  $L$  is defined as

$$P_L(\phi) = L^{\beta/\nu} \tilde{P}_L [\phi L^{\beta/\nu}] \quad (10)$$

where  $\tilde{P}_L$  is a scaling function. At the criticality, the distribution  $P_L(\phi)$  is unimodal for a continuous transition. The FSS form of the susceptibility is given by

$$\chi(\eta, L) = L^{\gamma/\nu} \chi_0[\epsilon L^{1/\nu}] \quad (11)$$

where  $\chi_0$  is a scaling function,  $\gamma/\nu = d - 2\beta/\nu$  and  $d$  ( $= 2$ ) is the space-dimension. At  $\eta = \eta_c$ ,  $\chi(\eta_c, L) \sim L^{\gamma/\nu}$ . The FSS form of the fourth order Binder cumulant is given by

$$U(\eta, L) = U_0[\epsilon L^{1/\nu}] \quad (12)$$

where  $U_0$  is a scaling function. The derivative of  $U(\eta, L)$  with respect to  $\eta$  follows a scaling relation [45],

$$U'(\eta, L) = L^{1/\nu} \frac{U'_0[\epsilon L^{1/\nu}]}{\eta_c} \quad (13)$$

where the primes on  $U$  and  $U_0$  denote their derivatives with respect to  $\eta$ . For a continuous transition, the cumulant  $U$  always remain positive. At  $\eta = \eta_c$ , the cumulants of different systems of size ( $L$ ) become independent of  $L$  and  $U'(\eta_c, L) \sim L^{1/\nu}$  at the transition.

In case the orientational order-disorder transition is discontinuous, the order parameter exponent  $\beta$  should go to zero. As a consequence, the susceptibility should then scale as  $\chi \sim L^d$ , where  $d$  is the space dimension. The Binder cumulant  $U$  would exhibit a sharp fall towards a negative value at the transition point. As the system exhibits the coexistence of two phases, the order parameter distribution  $P(\phi)$  would be a bimodal distribution.

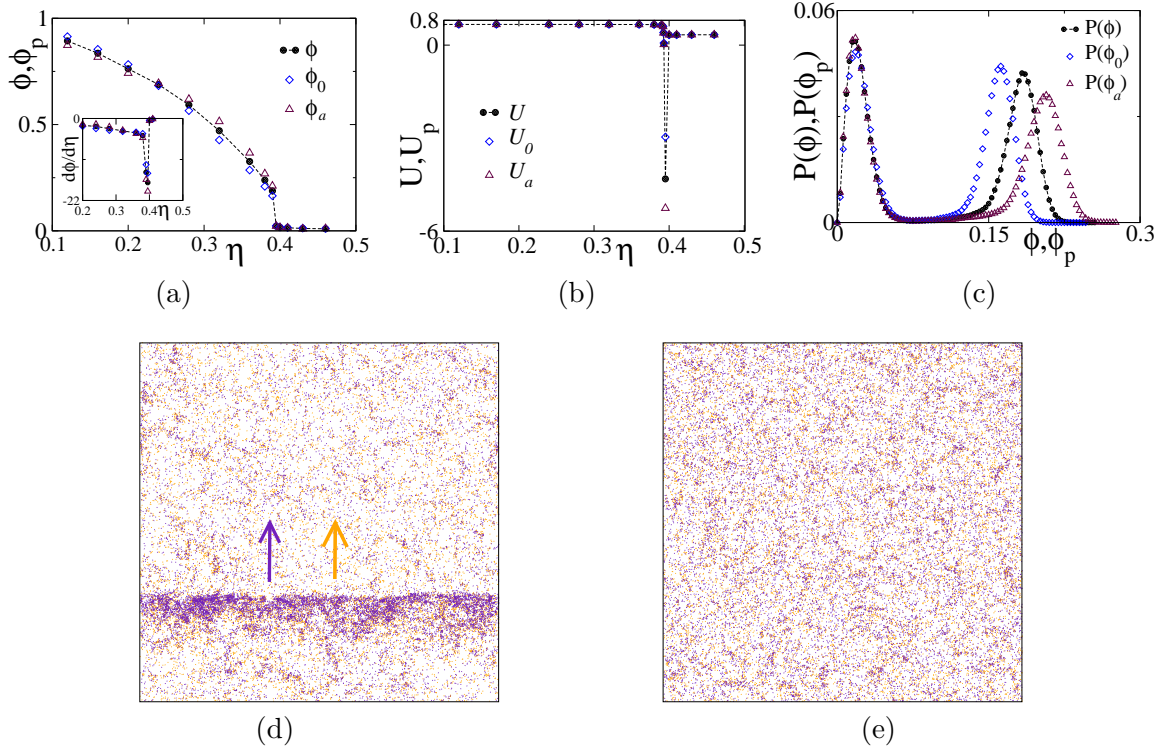


**Figure 2.** For  $v_0 = 1.0$ ,  $v_a = 1.2v_0$ : (a) Plot of  $\phi$  and  $\phi_p$  versus  $\eta$ . Derivatives of  $\phi$  and  $\phi_p$  with respect to  $\eta$  are shown in the inset. (b) Plot of  $U$  and  $U_p$  versus  $\eta$ . (c) Plot of  $P(\phi)$  and  $P(\phi_p)$  at  $\eta = \eta_c$ . System morphology for  $\eta \approx \eta_c$  with (d) ordered phase (density band) and (e) disordered phase. Orange colour represents the usual SPPs, and indigo colour represents the adapters. System size is  $L = 256$ .

#### 4. Results with different velocity ratios with fixed density ( $\rho_0 = \rho_a = 0.25$ )

Throughout the simulation, both the SPPs are kept in the same proportion as  $N_0 = N_a = N/2$ . The overall particle density  $\rho = N/L^2$  is fixed as  $\rho = 0.5$  for all the observations. One Monte Carlo (MC) time step corresponds to the up-gradation of the position and orientation of all the particles. Initial  $3 \times 10^5$  MC steps are neglected to achieve the steady state. An ensemble of size  $48 \times 10^5$  is taken for statistical averages ( $2 \times 10^5$  samples at different times for 24 different initial configurations). The results are shown with the velocity of the adapters as  $v_a > v_0$  for a fixed velocity of the usual SPPs  $v_0 = 1.0$ .

##### 4.1. Results with $v_a = 1.2v_0$ and $v_0 = 1.0$ :

First, we present data for  $\phi$  (and  $\phi_p$ ),  $U$  (and  $U_p$ ), and  $P(\phi)$  (and  $P(\phi_p)$ ) respectively in Fig.2(a), (b) and (c) on a system of size  $L = 256$  for  $v_a = 1.2v_0$ ,  $v_0 = 1.0$ . In this case, the velocity  $v_a$  of adapters is almost similar to the usual SPPs. The order parameter  $\phi$  of the whole system and  $\phi_p$ , that of the partial systems, are plotted against  $\eta$  in Fig.2(a). There are jumps in the values of  $\phi$  and  $\phi_p$  near the transition. The values of  $\phi$ ,  $\phi_0$  and  $\phi_a$  are almost similar for a given  $\eta$  in this case. The derivatives of  $\phi$  and  $\phi_p$  with respect to  $\eta$  are plotted in the inset of Fig.2(a) and sharp minima are observed at  $\eta_c \approx 0.39$  (same for the whole and the partial systems). The Binder cumulants  $U$  and  $U_p$  versus  $\eta$  plots are shown in Fig.2(b). The cumulant for the usual SPPs ( $U_0$ ), for adapters ( $U_a$ ) and for the whole system ( $U$ ) all show a sharp negative dip at the transition. It implies the discontinuous transition for the whole as well as for the partial systems. Then, the distributions of order parameters  $P(\phi)$  and  $P(\phi_p)$  at  $\eta = \eta_c$  are shown in Fig.2(c).

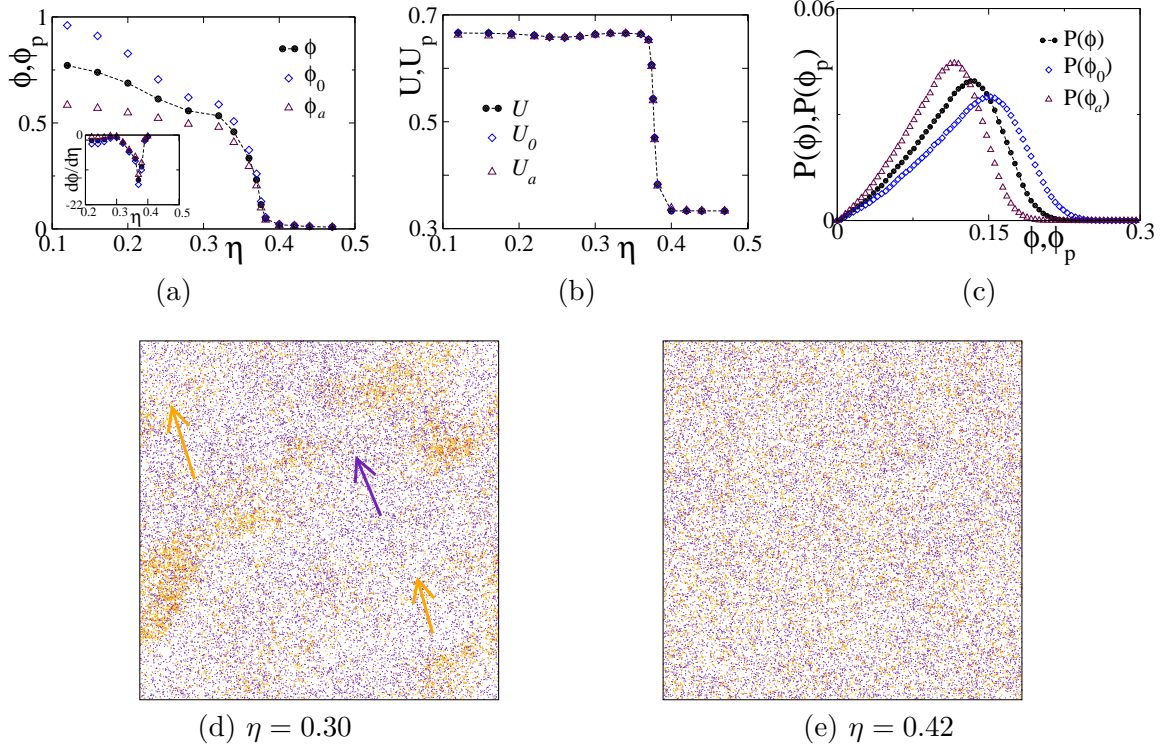


**Figure 3.** For  $v_0 = 1.0$ ,  $v_a = 7.0v_0$ : (a) Plot of  $\phi$  and  $\phi_p$  versus  $\eta$ . Derivatives of  $\phi$  and  $\phi_p$  with respect to  $\eta$  are shown in the inset. (b) Plot of  $U$  and  $U_p$  versus  $\eta$ . (c) Plot of  $P(\phi)$  and  $P(\phi_p)$  at  $\eta = \eta_c$ . System morphology for (d) ordered phase  $\eta = 0.30$  and (e) disordered phase  $\eta = 0.42$ . Orange colour represents the usual SPPs, and the indigo colour represents the adapters. System size is  $L = 256$ .

In this case, all three distributions  $P(\phi)$ ,  $P(\phi_0)$  and  $P(\phi_a)$  exhibit bimodal distributions, which implies the two-phase co-existence in the system.

The system morphology is shown in the ordered phase with  $\eta = 0.36$  and in the disordered phase with  $\eta = 0.40$ , respectively, in Fig.2(d) and (e). Near the transition, in the ordered phase (Fig.2(d)), both the adapters and usual SPPs are observed in the density band, and they move together in a particular direction (shown by arrows). This is expected as the adapters follow the usual SPPs; they move in the density band's direction. Moreover, their velocity is similar to the usual SPPs; they also form a dense band pattern near the usual SPPs. Whereas, at the disordered phase, no such dense band forms, and all the particles move randomly (Fig.2(e)). In the case of discontinuous transition, at the transition point, dense travelling bands of SPPs periodically form and disappear with time, resulting in the coexistence of two phases in the system. The situation will be different for a much higher velocity of the adapters.

#### 4.2. Results with $v_a = 7.0v_0$ and $v_0 = 1.0$ :

Next, the situation is going to be drastic if the velocity  $v_a$  is much higher than  $v_0$ . We present the data  $\phi$  (and  $\phi_p$ ),  $U$  (and  $U_p$ ), and  $P(\phi)$  (and  $P(\phi_p)$ ) respectively on a system of size  $L = 256$  for  $v_a = 7.0v_0$ ,  $v_0 = 1.0$  in Fig.3(a), (b) and (c), respectively. The order parameters  $\phi$  and  $\phi_p$ , are plotted against  $\eta$  in Fig.3(a). The order of the usual SPPs ( $\phi_0$ ) is higher than the order of adapters ( $\phi_a$ ) in the low  $\eta$  region in this case. However, near the transition, their values are similar. The values of  $\phi$  and  $\phi_p$  are decreasing smoothly to zero as  $\eta$  increases. The derivatives of  $\phi$  and  $\phi_p$  with respect to  $\eta$  are plotted in the inset of Fig.3(a) and minima of the plots at the

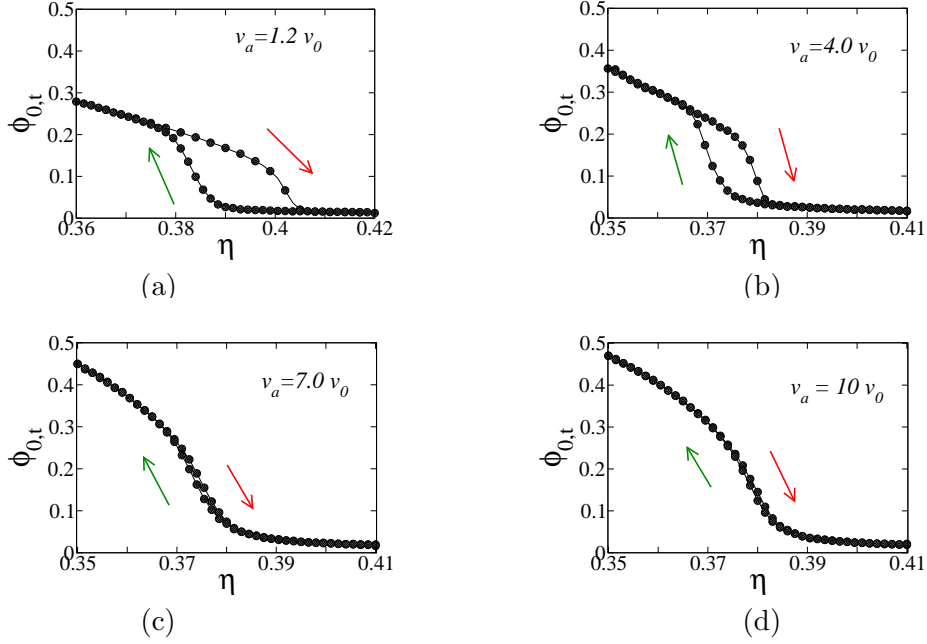


**Figure 4.** For  $v_a > v_0$ : Hysteresis plot for the usual SPPs with different values of adapter velocity as (a)  $v_a = 1.2v_0$ , (b)  $v_a = 4.0v_0$ , (c)  $v_a = 7.0v_0$  and (d)  $v_a = 10v_0$  with the fixed  $v_0 = 1.0$ . Results obtained by implementing ramp-up or forward (red arrow) and ramp-down or backward (green arrow) simulation schemes, respectively.

transition noise  $\eta_c \approx 0.37$  (same for the whole and partial systems) are observed. In Fig.3(b),  $U$  and  $U_p$  are plotted against  $\eta$ . Both  $U$  and  $U_p$  remain positive over the whole range of  $\eta$ . In Fig.3(c), the distribution of order parameters  $P(\phi)$  and  $P(\phi_p)$  are plotted at  $\eta = \eta_c$ . All the distributions are unimodal. The positive Binder cumulants and unimodal distributions of order parameters indicate a continuous transition in the whole system as well as in the partial systems for the case of  $v_a = 7.0v_0$  and  $v_0 = 1.0$ .

The system morphologies for the ordered phase with  $\eta = 0.30$  and for disordered phase with  $\eta = 0.42$  are shown in Fig.3(d) and (e) respectively for the case of  $v_a = 7.0v_0$  and  $v_0 = 1.0$ . Below the transition, at  $\eta = 0.30$  shown in Fig.3(d), less dense large clusters of usual SPPs are observed with small clusters of adapters, and they are directed in the same direction (shown by arrow). Whereas, above the transition, at  $\eta = 0.42$  shown in Fig.??(e), they move randomly. In this case, adapters move with much higher velocity and cannot flock with the usual SPPs. Moreover, they adopt the alignment information from usual SPPs, which are distant. It seems that as the usual SPPs interact with the adapters, randomness enters into the alignment of the usual SPPs. Hence, the correlation between the usual SPPs gets destroyed to form a dense band structure.

**Hysteresis study:** It is well known that the hysteresis phenomena usually accompany the first-order phase transition [23, 46, 47] which occurs near the transition. New simulations are carried out to measure the instantaneous order parameter ( $\phi_t$ ) by either gradually increasing or decreasing the angular noise  $\eta$  with a fixed ramp rate, where each previous state will be implemented as the initial state of the next simulation process with new  $\eta$ . The ramp rate used here is  $1.27 \times 10^{-6}$  in radians/unit time. Each hysteresis loop is obtained by averaging over 800 independent realizations. On ramping the angular noise parameter  $\eta$  at the same ramping rate up and down through the transition point, a hysteresis loop is formed in the case of the first-order phase transition and the loop area imply phase coexistence.

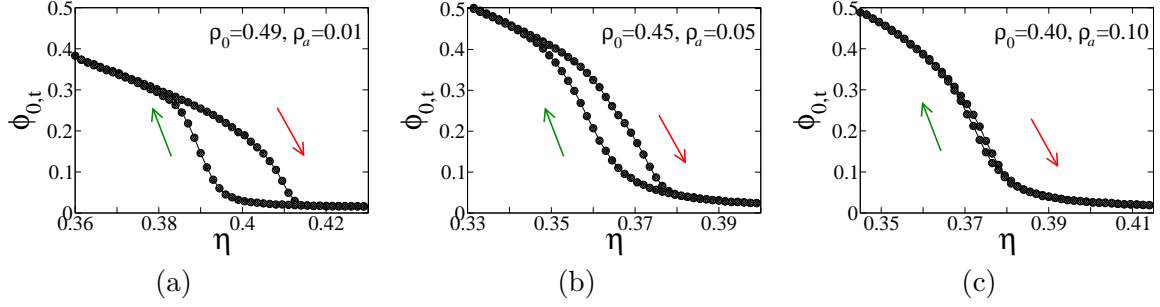


**Figure 5.** For  $v_a = 10v_0$ : Hysteresis plot for the usual SPPs with (a)  $\rho_0 = 0.49$ ,  $\rho_a = 0.01$ , (b)  $\rho_0 = 0.45$ ,  $\rho_a = 0.05$  and (c)  $\rho_0 = 0.40$ ,  $\rho_a = 0.10$ . Results obtained by implementing ramp-up or forward (red arrow) and ramp-down or backward (green arrow) simulation schemes, respectively.

Simulations are carried out to measure the instantaneous order parameter of the usual SPPs ( $\phi_{0,t}$ ) by either gradually increasing or decreasing  $\eta$  with a fixed ramp rate as discussed. The simulation results of hysteresis with different values of adapter's velocity as  $v_a = 1.2v_0$ ,  $4.0v_0$ ,  $7.0v_0$  and  $10v_0$  for a fixed  $v_0 = 1.0$ , are presented in Fig.4(a), (b), (c) and (d), respectively. Observations show that when  $v_a$  is relatively less as  $v_a = 1.2v_0$  with  $v_0 = 1.0$ , there arise an abrupt jump in the  $\phi_t$  and the positions of the jump by the implementation of the forward and backward simulations schemes are different. So the emergence of a hysteresis loop indicates the irreversibility of transition [23], shown in Fig.4(a). Hysteresis loop still exists for a moderately high value of  $v_a = 4.0v_0$  shown in Fig.4(b); however, it is less prominent than the  $v_a = 1.2v_0$  case. Then, for a large enough value of  $v_a = 7.0v_0$  and  $v_a = 10v_0$  the change of the order parameter versus  $\eta$  becomes reversible, which indicates continuous phase transition, as shown in Fig.4(c) and (d). It needs to be noted that similar behaviour of hysteresis plots for the different values of  $v_a$  is also observed for the whole system.

## 5. Results with different density ratio with $v_a = 10v_0$ ( $v_0 = 1.0$ )

As it is seen, the high velocity of the adapters induces a continuous transition when they are present in equal densities with the usual SPPs. For the fixed velocities of the two types  $v_a = 10v_0$  and  $v_0 = 1.0$ , we now see the effect of different density ratios on the collective behaviour. If  $\rho_a = 0$ , the model is equivalent to the VM ( $\rho_0 = 0.5$ ). Then a discontinuous order-disorder is expected to occur in the system for such  $v_0$ ,  $\rho_0$ . If the  $\rho_a$  is increased and  $\rho_0$  is decreased, keeping the total density fixed at 0.5, how it affects the transition is interesting to observe. For that, hysteresis is studied for different values of  $\rho_a$  and  $\rho_0$ . Simulations are carried out to measure the instantaneous order parameter of the usual SPPs ( $\phi_{0,t}$ ) by either gradually increasing or decreasing  $\eta$  with a fixed ramp rate as discussed earlier. The simulation results of hysteresis with different density ratios are presented in Fig.5, with the fixed velocities  $v_a = 10v_0$  and  $v_0 = 1.0$ . Observations show that when  $\rho_a = 0.01$  is relatively less, there arise an abrupt jump in the  $\phi_{0,t}$  and the positions of the jump by the implementation of the forward and backward simulations schemes are different, shown in Fig.5(a). Hysteresis loop still exists for an increase in the number of adapters as  $\rho_a = 0.05$  shown in Fig.5(b); however, it is less prominent than the  $\rho_a = 0.01$  case. Then, for a large enough value of  $\rho_a = 0.40$ , hysteresis disappears, and the change of the order parameter versus  $\eta$  becomes reversible, which indicates continuous phase transition, shown in Fig.5(c). It needs to be noted that similar behaviour of hysteresis plots for the different values of  $\rho_a$  is also observed for the whole system.



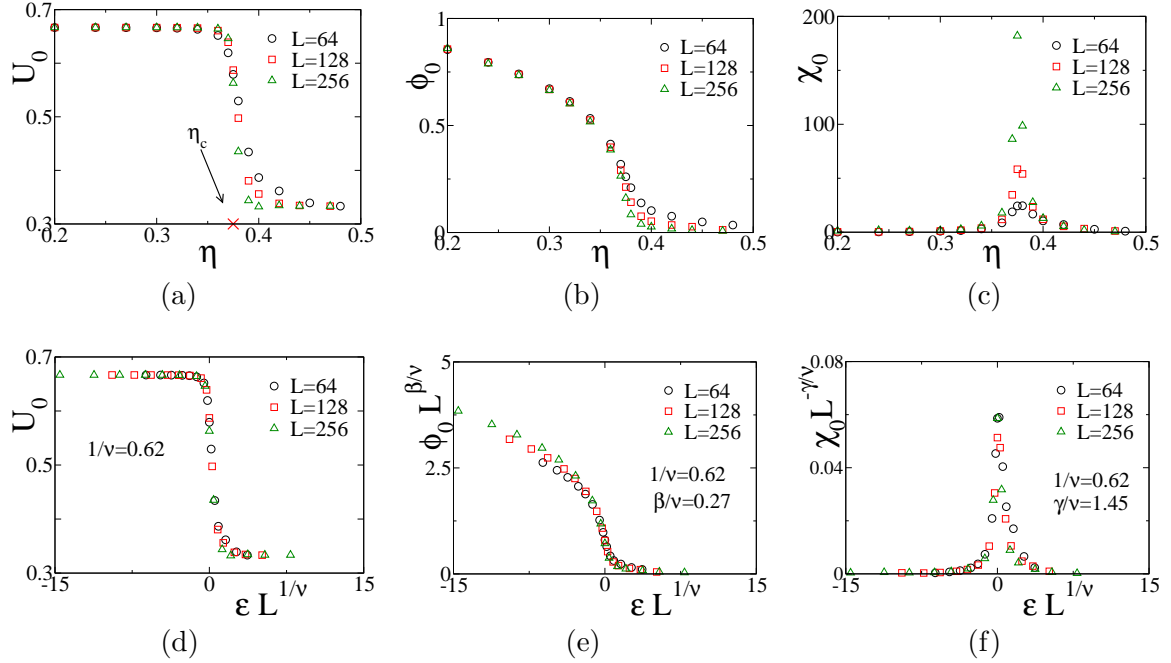


**Figure 6.**  $v_a = 10v_0$ ,  $\rho_0 = 0.40$ ,  $\rho_a = 0.10$ : (a) Plot of  $U_0$ , (b)  $\phi_0$  and (c)  $\chi_0$  versus  $\eta$  for  $L = 64, 128$  and  $256$ . In plot (a), the cross on the  $\eta$ -axis indicates  $\eta_c$ . (d) Plot of  $U_0$  versus the scaled noise  $\epsilon L^{1/\nu}$ . (e) Plot of  $\phi_0 L^{\beta/\nu}$  against  $\epsilon L^{1/\nu}$ . (f) Plot of  $\chi_0 L^{-\gamma/\nu}$  against  $\epsilon L^{1/\nu}$ . The values of the exponents are taken as  $\beta/\nu = 0.27$ ,  $\gamma/\nu = 1.45$  and  $1/\nu = 0.62$ .

### 5.1. Finite-size scaling analysis:

The critical exponents are extracted for the usual particles with  $v_a = 10v_0$  and  $\rho_0 = 0.40$ ,  $\rho_a = 0.10$  performing FSS analysis. Binder cumulant  $U_0$ , order parameter  $\phi_0$  and susceptibility  $\chi_0$  are plotted against the angular noise  $\eta$  for three different systems of sizes  $L = 64, 128$  and  $256$  in Fig.6(a), (b) and (c) respectively. The plots of  $U_0$  versus  $\eta$  for different  $L$  intersect at  $\eta_c \approx 0.37$ , the  $L$  independent critical point as expected in a continuous transition. It is marked by a cross on the  $\eta$ -axis. A rough estimate of the exponents  $1/\nu$ ,  $\beta/\nu$  and  $\gamma/\nu$  are obtained from the scaling relations  $U_0'(\eta_c, L) \sim L^{1/\nu}$ ,  $\phi_0(\eta_c, L) \sim L^{-\beta/\nu}$  and  $\chi_0(\eta_c, L) \sim L^{\gamma/\nu}$  at the criticality. The best possible FSS forms of the scaled parameters against the scaled noise  $\epsilon L^{1/\nu}$  are obtained, tuning these exponents further.  $U_0$ ,  $\phi_0 L^{\beta/\nu}$ , and  $\chi_0 L^{-\gamma/\nu}$  are plotted against  $\epsilon L^{1/\nu}$  in Fig.6(d), (e) and (f), respectively. A reasonable collapse of data in all three cases is obtained by taking  $1/\nu = 0.62$ ,  $\beta/\nu = 0.27$  and  $\gamma/\nu = 1.45$  at  $\eta_c = 0.37$ . The critical exponents satisfy the scaling relation  $\gamma/\nu + 2\beta/\nu = 2$  within error bars. The exponents are similar to the exponents for the VM [48] with  $v_0 = 0.1$  and density  $\rho = 1/8$  to  $3/4$ .

## 6. Summary and Discussion

In this work, the collective motion of a mixture of usual SPPs and orientation adapters is modelled. The two species have different velocities. The adapters have higher velocity than the usual SPPs, while the velocity of the usual SPPs is fixed at a high velocity  $v_0 = 1.0$ . For the same density of the two species, with the adapter velocity  $v_a = 1.2v_0$ , both adapters and the usual SPPs form dense travelling bands in the system. Both the travelling bands move in the same direction in accordance with the orientation rule. Near the transition point, such bands appear and disappear over time, giving rise to co-existence of two phases. The adapters and the usual SPPs both undergo a discontinuous transition characterized by a negative dip in the Binder

cumulant and bimodal distribution of order parameters. The nature of the transition is further confirmed by the existence of hysteresis in the order parameter under a continuously varying noise field. This is quite expected in the context of the VM. However, more dramatic effects are revealed as the adapter velocity becomes much higher than the usual SPPs. Surprisingly, the formation of travelling bands disappears from the system. In the ordered phase, the flocks of usual SPPs form directed clusters, and the adapters form relatively smaller directed clusters. All these clusters move in the same direction as expected. In the disordered phase ( $\eta > \eta_c$ ), these clusters melt into smaller clusters and move randomly. Consequently, continuous transitions occur for both the adapters and the usual SPPs, even at such high velocities. The continuous transitions are characterized by positive Binder cumulant and unimodal distribution of the order parameter. The hysteresis loops also disappear for these systems. Such continuous transition is also observed even for a smaller fraction of adapters ( $\rho_a = 0.10$ ,  $\rho_0 = 0.40$ ) with high velocity  $v_a = 10v_0$ . Furthermore, the values of critical exponents related to the continuous transitions are determined. In this system, the alignment of an adapter obtained from local interaction may be very different from the alignment of SPPs at a distant point where the adapter moves after position update due to its high velocity. Such misalignment in orientations between the adapters and the SPPs introduces extra fluctuations in the system. Such fluctuations grow predominantly in the transition region, and all long-range correlations get destroyed. The continuous nature of the transition is essentially a manifestation of such a smooth crossover from a correlated system to an uncorrelated system.

**Acknowledgement:** The computational facility HPC Newton and Param-Ishan provided by the Department of Physics, Indian Institute of Technology Guwahati is gratefully acknowledged.

## References

- [1] Becco C, Vandewalle N, Delcourt J and Poncin P 2006 *Physica A* **367** 487–493
- [2] Makris N C, Ratilal P, Jagannathan S, Gong Z, Andrews M, Bertatos I, Godø O R, Nero R W and Jech J M 2009 *Science* **323** 1734–1737
- [3] Filella A, Nadal F, Sire C, Kanso E and Eloy C 2018 *Physical review letters* **120** 198101
- [4] Ballerini M, Cabibbo N, Candelier R, Cavagna A, Cisbani E, Giardina I, Lecomte V, Orlandi A, Parisi G, Procaccini A, Viale M and Zdravkovic V 2008 *Proc. Natl. Acad. Sci. U.S.A.* **105** 1232–1237
- [5] Cavagna A, Cimarelli A, Giardina I, Parisi G, Santagati R, Stefanini F and Viale M 2010 *Proc. Natl. Acad. Sci. U.S.A.* **107** 11865–11870
- [6] Ginelli F, Peruani F, Pillot M H, Chaté H, Theraulaz G and Bon R 2015 *Proceedings of the National Academy of Sciences* **112** 12729–12734
- [7] Helbing D, Farkas I and Vicsek T 2000 *Nature* **407** 487–490
- [8] Helbing D, Johansson A and Al-Abideen H Z 2007 *Physical review E* **75** 046109
- [9] Kelley D H and Ouellette N T 2013 *Scientific reports* **3** 1073
- [10] Okubo A and Chiang H 1974 *Population Ecology* **16** 1–42
- [11] Buhl J, Sumpter D J, Couzin I D, Hale J J, Despland E, Miller E R and Simpson S J 2006 *Science* **312** 1402–1406
- [12] Romanczuk P, Couzin I D and Schimansky-Geier L 2009 *Phys. Rev. Lett.* **102** 010602
- [13] Shapiro J A 1998 *Annual review of microbiology* **52** 81–104
- [14] Zhang H, Be’Er A, Smith R S, Florin E L and Swinney H L 2009 *EPL (Europhys. Lett.)* **87** 48011
- [15] Zhang H P, Be’er A, Florin E L and Swinney H L 2010 *Proceedings of the National Academy of Sciences* **107** 13626–13630
- [16] Malet-Engra G, Yu W, Oldani A, Rey-Barroso J, Gov N S, Scita G and Dupré L 2015 *Current Biology* **25** 242–250
- [17] Schaller V, Weber C, Semmrich C, Frey E and Bausch A R 2010 *Nature* **467** 73–77
- [18] Sanchez T, Chen D T, DeCamp S J, Heymann M and Dogic Z 2012 *Nature* **491** 431–434
- [19] Vicsek T and Zafeiris A 2012 *Phys. Rep.* **517** 71–140
- [20] Shaebani M R, Wysocki A, Winkler R G, Gompper G and Rieger H 2020 *Nat Rev Phys* **2** 181–199
- [21] Morin A, Desreumaux N, Caussin J B and Bartolo D 2017 *Nature Physics* **13** 63–67
- [22] Nagy M, Daruka I and Vicsek T 2007 *Physica A* **373** 445–454
- [23] Chaté H, Ginelli F, Grégoire G and Raynaud F 2008 *Phys. Rev. E* **77** 046113
- [24] Adhikary S and Santra S B 2021 *Europhys. Lett.* **135** 48003

- [25] Ginelli F 2016 *Eur. Phys. J. Special Topics* **225** 2099–2117
- [26] Adhikary S and Santra S B 2022 *Journal of Physics: Conference Series* **2207** 012023
- [27] Adhikary S and Santra S 2022 *Phys. Rev. E* **105** 064612
- [28] Mishra S, Tunström K, Couzin I D and Huepe C 2012 *Phys. Rev. E* **86** 011901
- [29] Singh J P and Mishra S 2020 *Physica A* **544** 123530
- [30] Dolai P, Simha A and Mishra S 2018 *Soft Matter* **14** 6137–6145
- [31] Weber S N, Weber C A and Frey E 2016 *Phys. Rev. Lett.* **116** 058301
- [32] Kumari S, Nunes A S, Araújo N A and Telo da Gama M M 2017 *The Journal of chemical physics* **147** 174702
- [33] Stenhammar J, Wittkowski R, Marenduzzo D and Cates M E 2015 *Phys. Rev. Lett.* **114** 018301
- [34] Maloney R C and Hall C K 2020 *Langmuir* **36** 6378–6387
- [35] McCandlish S R, Baskaran A and Hagan M F 2012 *Soft Matter* **8** 2527–2534
- [36] Menzel A M 2012 *Phys. Rev. E* **85**(2) 021912
- [37] Reichhardt C, Thibault J, Papanikolaou S and Reichhardt C 2018 *Phys. Rev. E* **98** 022603
- [38] Ikeda M, Wada H and Hayakawa H 2012 *EPL (Europhysics Letters)* **99** 68005
- [39] Bain N and Bartolo D 2017 *Nature communications* **8** 1–6
- [40] Ai B Q, Shao Z G and Zhong W 2018 *Soft Matter* **14**
- [41] Liebchen B and Levis D 2017 *Phys. Rev. Lett.* **119** 058002
- [42] Sampat P B and Mishra S 2021 *Phys. Rev. E* **104** 024130
- [43] Binder K 1987 *Reports on progress in physics* **50** 783
- [44] Christensen K and Moloney N R 2005 *Complexity and criticality* vol 1 (World Scientific Publishing Company)
- [45] Cambui D S, de Arruda A S and Godoy M 2016 *Physica A* **444** 582–588
- [46] Durve M and Sayeed A 2016 *Phys. Rev. E* **93** 052115
- [47] Li B, Wu Z X and Guan J Y 2019 *Phys. Rev. E* **99**(2) 022609
- [48] Baglietto G and Albano E V 2008 *Phys. Rev. E* **78** 021125